SPANDIDOS PUBLICATIONS

ONCOLOGY LETTERS 17: 2283-2295, 2019

Identification of imatinib-resistant long non-coding RNAs in gastrointestinal stromal tumors

JINGYI YAN[1*], DIDI CHEN[2*], XIAOLEI CHEN[1], XUECHENG SUN[3], QIANTONG DONG[1], ZHOU DU[1] and TINGTING WANG[2]

Departments of [1]Gastroenterology and General Surgery, [2]Radiotherapy and Medical Oncology, and [3]Gastroenterology and Hepatology, The First Affiliated Hospital of Wenzhou Medical University, Wenzhou, Zhejiang 325000, P.R. China

Received November 9, 2017; Accepted November 6, 2018

DOI: 10.3892/ol.2018.9821

Abstract. Long non-coding RNAs (lncRNAs) are an abundant RNA species that belong to the competing endogenous RNA network, which serves a critical role in the development, diagnosis and progression of diseases. Using chip technology, the current study analyzed the expression of lncRNAs in paired normal gastric tissues, primary gastrointestinal stromal tumor (GIST) tissues and GIST tissues resistant to imatinib mesylate. Gene Ontology enrichment and Kyoto Encyclopedia of Genes and Genomes pathway analyses were used to predict potential tumorigenesis and drug resistance mechanisms. The hypoxia-inducible factor-1 pathway was identified as a putative mediator of drug resistance. To the best of our knowledge, the current study was the first to investigate the role of lncRNAs in imatinib mesylate-resistant GISTs and primary GISTs using chip technology. An association was revealed between lncRNA expression and imatinib mesylate resistance. In summary, the current study identified a panel of dysregulated lncRNAs that may serve as potential biomarkers or drug targets for GISTs, particularly secondary imatinib-resistant GISTs.

Correspondence to: Dr Xiaolei Chen, Department of Gastroenterology and General Surgery, The First Affiliated Hospital of Wenzhou Medical University, Nanbaixiang, Ouhai, Wenzhou, Zhejiang 325000, P.R. China
E-mail: cxlei0918@sina.com

*Contributed equally

Abbreviations: lncRNA, long non-coding RNA; GIST, gastrointestinal stromal tumor; HIF-1, hypoxia-inducible factor-1; IM, imatinib mesylate; N, normal gastric tissue; Y, primary gastrointestinal stromal tumor tissue; C, gastrointestinal stromal tumor tissue secondarily resistant to imatinib mesylate

Key words: long non-coding RNAs, gastrointestinal stromal tumor, hypoxia-inducible factor-1, imatinib mesylate resistance

Introduction

Gastrointestinal stromal tumors (GISTs) are a distinct type of tumor with the highest incidence among sarcomas of the gastrointestinal tract in humans (1). GISTs account for 2.2% of the morbidity associated with malignant tumors of the gastrointestinal tract (2). Although imatinib mesylate (IM) has been revolutionary in the treatment of advanced GISTs, clinical resistance to IM is an issue for patients that require prolonged treatment (3,4).

Long non-coding RNAs (lncRNAs) have been demonstrated to mediate a number of pathophysiological processes. lncRNAs are key regulators of important biological processes involved in development and differentiation (5,6). Previous studies have identified that lncRNAs exhibit active roles in modulating the cancer epigenome and may be important targets for cancer diagnosis and therapy (7-11). It has been revealed that lncRNAs may promotes GIST progression and metastasis (12). The lncRNA HOX transcript antisense RNA (HOTAIR) is upregulated in GISTs and can promote GIST cell invasiveness *in vitro* (13). Using a gene microarray, Lee *et al* (13) identified that protocadherin 10 (PCDH10) is a key target of HOTAIR. HOTAIR could regulate promoter methylation of PCDH10 and promote GIST cell invasion and migration. However, to the best of our knowledge, little is known regarding the role of other lncRNAs in GIST.

Imatinib is the first line of therapy for patients with metastatic or end-stage GISTs; however, drug resistance limits the long-term curative effect of imatinib (14,15). Numerous studies have demonstrated that lncRNAs, including urothelial carcinoma-associated 1 and HOTAIR, serve a role in promoting acquired resistance to imatinib in chronic myeloid leukemia cells (16,17). lncRNAs also serve an important role in regulating imatinib resistance in GISTs, CCDC26 lncRNA knockdown can induce imatinib resistance in GIST cells by downregulating c-KIT expression (18). It has been identified that the malignant character of GISTs is initiated and amplified by PCDH10 in a process regulated by HOTAIR lncRNA (13).

The aim of the current study was to screen differentially expressed lncRNAs associated with GISTs and IM secondary resistance. This screening was performed to identify candidate

lncRNAs that may serve as targets for reversing drug resistance or as biomarkers for predicting and preventing imatinib secondary resistance.

Materials and methods

Clinical samples. Tumor tissues (≥5 cm) and normal gastric tissues were obtained from 9 patients (mean, 56; range, 39-70-years), 4 male and 5 female, who underwent surgical resection between December 2015 and August 2016 at The First Affiliated Hospital of Wenzhou Medical University (Zhejiang, China). Tissue samples included three normal gastric tissue samples (N), three primary GIST samples (Y or YC) and three GIST samples secondarily resistant to IM (C). The GIST samples included the standard resection of GISTs performed on these patients, and treatment with a 400-mg daily dose of imatinib was applied for the postoperative period. These patients underwent surgery again owing to GIST recurrence, and the daily dose of imatinib was increased to 800 mg, postoperatively. A third surgical resection was carried out owing again to GIST recurrence and these samples were collected. The current study was approved by the Ethics Committee of The First Affiliated Hospital of Wenzhou Medical University and informed written consent was obtained from the patients prior to surgery.

Immunohistochemistry analysis. All tumor tissues were confirmed to be malignant GISTs by pathological examination and immunohistochemistry ($CD117^+$, $CD34^+$, mitotic phase >5/50 high-power field). Paraffin-embedded tissues (thickness, 3.5 μg) were fixed with 10% formalin at 23-26˚C for 12-24 h. Tissues were subsequently incubated with CD117 rabbit anti-human antibody (dilution 1:800; cat. no., Kit-0029; Fuzhou Maixin Biotech Co., Ltd., Fuzhou, China) and CD34 rat anti-human antibody (dilution 1:600; cat. no., Kit-0004; Fuzhou Maixin Biotech Co., Ltd.) incubated overnight at 4˚C. Sections were subsequently inclubated with secondary antibody peroxidase-labelled polymer conjugated to goat antirabbit IgG (dilution, 1:500; cat. no., Kit-0014; Fuzhou Maixin Biotech Co., Ltd.) sections were incubated for 30 min at 37˚C. All samples were stored in liquid nitrogen until further experiments.

RNA extraction and chip hybridization. The MirVanaTM RNA Isolation kit (Thermo Fisher Scientific, Inc., Waltham, MA, USA) was used for RNA extraction from the 9 tissue samples. The total RNA was quantified using a NanoDrop ND-2000 (Thermo Fisher Scientific, Inc.) and the integrity of the RNA was determined using an Agilent 2100 Bioanalyzer system (Agilent Technologies, Inc., Santa Clara, CA, USA). The microarray experiments were performed by OeBiotech Corporation (Shanghai, China). The Human OE lncRNA Microarray Technology (Affymetrix; Thermo Fisher Scientific, Inc.), which contains 63,542 lncRNAs and 27,134 mRNAs, was used. The sample labeling, microarray hybridization and washing were performed according to the manufacturer's protocol. Briefly, the total RNA was transcribed into double-stranded complementary DNA (cDNA) and then synthesized into complementary RNAs (cRNA). Subsequently, second-cycle cDNAs were synthesized from the cRNAs. Following fragmentation and biotin labeling, the second-cycle cDNAs were hybridized onto the microarray. Following washing and staining, the arrays were scanned on the GeneChip Scanner 3000 system (Affymetrix; Thermo Fisher Scientific, Inc.).

Data analysis. Data extraction and standardization were performed using GeneSpring GX 13.1 software (Agilent Technologies, Inc.). Differentially expressed genes and lncRNAs were screened using an unpaired Student's t-test. The cut-off criteria for selecting differentially expressed mRNAs and lncRNAs was a fold-change (FC) in expression of ≥2.0 and P≤0.05. Hierarchical clustering was performed using GeneSpring GX 11.5.1 software (Agilent Technologies, Inc.). Subsequently, Gene Ontology (GO) enrichment and Kyoto Encyclopedia of Genes and Genomes (KEGG) pathway analysis was performed to determine the putative roles of the differentially expressed mRNAs and lncRNAs.

Co-expression analysis of lncRNAs and mRNAs. The co-expression of the differentially expressed lncRNAs and mRNAs was evaluated by Pearson's correlation coefficient analysis. P≤0.05 and a correlation coefficient of >0.7 indicated a statistically significant correlation between the expression of lncRNA and mRNA. The overlap of the co-expressed mRNA set and the transcription factor (TF) target gene set was calculated based on the hypergeometric distribution. The TFs used for analysis were obtained from database ENCODEPROJECT (https://www.encodeproject.org/), and the method refers to the TF enrichment analysis in DAVID database (https://david.ncifcrf.gov/). If the co-expressed mRNAs of the given lncRNAs overlapped with the target genes of the given TFs, the TFs were considered to be interacting with the lncRNAs. The lncRNA-TF-mRNA interactions were used to construct networks using Cytoscape (version 3.11; cytoscape.org). The function of each lncRNA co-expressed with an mRNA was analyzed using GO enrichment and KEGG pathway analyses based on hypergeometric distribution.

Quantitative analysis. Reverse transcription-quantitative polymerase chain reaction (RT-qPCR) was used to validate 6 lncRNAs by random selection. Total RNA was extracted from cancer tisuss using TRIzol™ Reagent (Invitrogen; Thermo Fisher Scientific, Inc.). First-strand cDNA was generated using a Reverse Transcription System kit (Promega Corporation, Madison, WI, USA), according to the manufacturer's protocols. Quantification was performed with a two-step reaction process: RT and PCR. Each RT reaction consisted of two steps.The first step was 0.5 μg RNA, 2 μl of 4X gDNA wiper Mix and the addition of nuclease-free H_2O to 8 μl. Reactions were performed in a GeneAmp® PCR System 9700 (Applied Biosystems; Thermo Fisher Scientific, Inc.) for 2 min at 42˚C. The second step was adding 2 μl of 5X HiScript II Q RT SuperMix IIa. Reactions were performed in a GeneAmp® PCR System 9700 (Applied Biosystems; Thermo Fisher Scientific, Inc.) for 10 min at 25˚C; 30 min at 50˚C and 5 min at 85˚C. The 10 μl RT reaction mix was subsequently diluted x 10 in nuclease-free water and held at -20˚C for 10 sec. Reactions were incubated in a 384-well optical plate (Roche Diagnostics)

Table I. Primer sequences used for reverse transcription-quantitative polymerase chain reaction.

lncRNA	Direction	Primer sequences
lnc-TERT-2	Forward	5'-GTGAACTACAAGGTAAGGCG-3'
	Reverse	5'-ACTTCAACTGAAACAGGAGAG-3'
lnc-OMD-1	Forward	5'-TCTTCCTCCCAAGCTCAC-3'
	Reverse	5'-GCTGAATGAGCCTAATAGGATG-3'
lnc-ATP7A-2	Forward	5'-CAAAGCTCTCATGGATGAGG-3'
	Reverse	5'-CTGCCAGCTTATATGGGTATT-3'
lnc-TCF4-6	Forward	5'-TATGGCAAATCTGCCTGTTCA-3'
	Reverse	5'-GCCTCATAGACAATGGATACGA-3'
lnc-RERE-4	Forward	5'-CATAATTCTAACCTGCCCGC-3'
	Reverse	5'-TTCTTCAAAGGTCCAGAGAGT-3'
lnc-SNRPN-2	Forward	5'-ACTTTTTGAGTGCATAAGGGT-3'
	Reverse	5'-ACTTCAAACACTGTATCCTCAA-3'
lnc-FAM108B1-3	Forward	5'-GCTACTTCCCTATTCTGAAAAG-3'
	Reverse	5'-TGACCCATGTGTTTCAATTCC-3'
ACTB	Forward	5'-CCATCATGAAGTGTGACG-3'
	Reverse	5'-GCCGATCCACACGGAGTA-3'

lncRNA, long non-coding RNA.

Table II. Top ten differentially expressed mRNAs for each comparison.

Gene symbol	P-value	Fold-change	Regulation
C vs. N			
DPP10	7.85×10^{-6}	3,029.7207	Upregulated
CSRP1	2.43×10^{-5}	1,280.9022	Downregulated
TPM1	1.21×10^{-4}	465.1485	Downregulated
PALLD	9.82×10^{-5}	463.9496	Downregulated
KIT	1.04×10^{-5}	454.6385	Upregulated
PLAT	5.23×10^{-5}	415.0655	Upregulated
ANO1	9.09×10^{-6}	397.9115	Upregulated
SLMAP	1.18×10^{-5}	372.9152	Downregulated
MYL9	6.12×10^{-5}	258.0424	Downregulated
RGS5	3.75×10^{-4}	226.5819	Downregulated
C vs. Y			
OGN	3.51×10^{-4}	731.1902	Upregulated
CLPTM1L	3.42×10^{-4}	157.8434	Upregulated
LDHA	2.51×10^{-3}	83.7515	Upregulated
TM4SF1	9.60×10^{-4}	69.0364	Upregulated
BHLHE40	3.76×10^{-5}	67.7466	Upregulated
MT1X	2.60×10^{-3}	52.4122	Upregulated
MT2A	2.42×10^{-3}	49.3582	Upregulated
C7	5.81×10^{-3}	45.7806	Upregulated
SPP1	3.40×10^{-3}	39.3369	Upregulated
TMEM45A	2.78×10^{-4}	38.8151	Upregulated
Y vs. N			
DPP10	9.41×10^{-6}	2,421.0703	Upregulated
CNN1	3.59×10^{-4}	1,231.3666	Downregulated
MYH11	1.04×10^{-3}	1,125.5151	Downregulated
TPM1	2.88×10^{-4}	589.9242	Downregulated
PALLD	5.93×10^{-6}	583.9103	Downregulated
PLAT	7.13×10^{-5}	558.9153	Upregulated
ANO1	2.64×10^{-6}	457.2661	Upregulated
F2RL2	3.66×10^{-4}	436.2676	Upregulated
KIT	8.03×10^{-6}	372.8208	Upregulated
SORBS1	5.04×10^{-4}	354.0606	Downregulated

N, normal gastric tissue samples; Y, primary gastrointestinal stromal tumor samples; C, imatinib mesylate-resistant gastrointestinal stromal tumor samples.

at 95˚C for 5 min, followed by 40 cycles of 95˚C for 10 sec, 60˚C for 30 sec. Each sample was run in triplicate for analysis. At the end of the PCR cycles, melting curve analysis was performed to validate the specific generation of the expected PCR product. The PCR was performed using the SYBR Green Premix DimerEraser kit (Takara Bio, Inc., Otsu, Japan) on the Roche LightCycler 480 Instrument II (Roche Diagnostics) with 10 μl PCR reaction mixture that included 1 μl of cDNA, 5 μl of 2X QuantiFast® SYBR® Green PCR Master Mix (Qiagen GmbH, Hilden, Germany), 0.2 μl of forward primer, 0.2 μl of reverse primer and 3.6 μl of nuclease-free water. The relative gene expression was analyzed using the $2^{-\Delta\Delta Cq}$ method (19). Primer sequences are presented in Table I.

Statistical analysis. All experimental data were presented as the mean ± standard deviation and analyzed using GraphPad Prism 5.0 software (GraphPad Software, Inc., La Jolla, CA, USA). Significance was analyzed using an unpaired Student's t-test. $P<0.05$ was considered to indicate a statistically significant difference.

Results

Differentially expressed mRNAs and lncRNAs. Differentially expressed mRNAs and lncRNAS were selected according to the following criteria: FC ≥2.0 and P≤0.05 (Tables II and III). Volcano plots, containing differentially expressed mRNAs and lncRNAs, were generated based on the P-values and FC values, and were used to demonstrate the differentially

Table III. Top ten differentially expressed lncRNAs for each comparison.

Gene symbol	P-value	Fold-change	Regulation
C vs. N			
lnc-FADD-2	$3.54x10^{-6}$	374.60214	Upregulated
lnc-TERT-2	$1.77x10^{-5}$	326.4259	Upregulated
lnc-LPP-2	$9.15x10^{-6}$	227.83163	Downregulated
lnc-PHLDA3-3	$1.38x10^{-5}$	213.00255	Downregulated
lnc-GPR108-2	$3.20x10^{-4}$	99.080215	Downregulated
lnc-DIRC3-4	$1.65x10^{-5}$	91.854065	Downregulated
lnc-C3orf80-3	$5.60x10^{-6}$	79.911095	Upregulated
lnc-C11orf89-3	$7.06x10^{-5}$	77.44088	Upregulated
lnc-CFH-2	$2.51x10^{-4}$	74.221596	Upregulated
lnc-CFHR3-1	$1.31x10^{-5}$	71.0337	Upregulated
C vs. Y			
lnc-TERT-2	$5.72x10^{-5}$	169.64801	Upregulated
lnc-OMD-1	$7.32x10^{-4}$	95.35182	Upregulated
lnc-ATP7A-2	$7.29x10^{-6}$	31.169392	Upregulated
lnc-TCF4-6	$2.13x10^{-3}$	23.001923	Downregulated
lnc-RERE-4	$6.76x10^{-4}$	21.957548	Upregulated
lnc-TCP1-5	$3.99x10^{-3}$	20.307957	Upregulated
lnc-SNRPN-2//RP11-701H24.7//NONHSAG016304	$2.28x10^{-2}$	18.521355	Downregulated
lnc-FAM108B1-3	$7.44x10^{-4}$	17.824202	Upregulated
lnc-C15orf54-4//CTD-2033D15.2//NONHSAG016560	$1.04 x10^{-2}$	15.087145	Upregulated
lnc-ATP7A-1	$2.44x10^{-4}$	14.85991	Upregulated
Y vs. N			
lnc-SIDT2-1	$4.30x10^{-4}$	610.91364	Downregulated
lnc-FADD-2	$2.85x10^{-6}$	597.95306	Upregulated
lnc-RP1-177G6.2.1-2	$1.50x10^{-7}$	522.8559	Downregulated
lnc-DYNC2LI1-1	$1.60x10^{-6}$	469.5526	Upregulated
CDR1-AS//lnc-RP1-177G6.2.1-3//NONHSAG055442	$1.89x10^{-11}$	196.92441	Downregulated
lnc-LPP-2	$3.19x10^{-5}$	175.79048	Downregulated
lnc-C11orf89-3	$2.42x10^{-5}$	146.4682	Upregulated
lnc-RPH3AL-2	$2.29x10^{-4}$	146.42218	Upregulated
lnc-CFH-2	$4.91x10^{-5}$	116.60803	Upregulated
lnc-SLC27A6-3	$2.86x10^{-5}$	104.92543	Upregulated

lncRNA, long non-coding RNA; N, normal gastric tissue samples; Y, primary gastrointestinal stromal tumor samples; C, imatinib mesylate-resistant gastrointestinal stromal tumor samples.

expressed mRNAs and lncRNAs between two groups of data (Fig. 1).

As presented in Table IV, 3,070 differentially expressed mRNAs were identified between group C and N, including 1,836 upregulated mRNAs and 1,234 downregulated mRNAs. In addition, 2,209 differentially expressed lncRNAs were revealed between group C and N, including 1,299 upregulated lncRNAs and 910 downregulated lncRNAs. Between group C and Y, 1,315 differentially expressed mRNAs were identified, including 933 upregulated mRNAs and 382 downregulated mRNAs. In addition, 922 lncRNAs were differentially expressed between group C and Y, including 493 upregulated lncRNAs and 429 downregulated lncRNAs. Between group Y and N, 2,712 differentially expressed mRNAs were revealed, including 1,213 upregulated mRNAs and 1,499 downregulated mRNAs. Between group Y and N, 2,250 lncRNAs were identified to be differentially expressed, including 1,241 upregulated lncRNAs and 1,009 downregulated lncRNAs.

Cluster analysis of differentially expressed mRNAs and lncRNAs. Hierarchical clustering was performed to reveal the distinguishable gene expression patterns among samples (Fig. 2). Between the two groups (C vs. N; C vs. Y and Y vs. N), a common set of downregulated and upregulated genes were identified. The common differentially expressed genes may be involved in the mechanisms of oncology and secondary resistance.

Table IV. Results of differential screening.

	mRNA			lncRNA		
Comparison	Total, n	Upregulated, n	Downregulated, n	Total, n	Upregulated, n	Downregulated, n
C vs. N	3,070	1,836	1,234	2,209	1,299	910
C vs. Y	1,315	933	382	922	493	429
Y vs. N	2,712	1,213	1,499	2,250	1,241	1,009

lncRNA, long non-coding RNA; N, normal gastric tissue samples; Y, primary gastrointestinal stromal tumor samples; C, imatinib mesylate-resistant gastrointestinal stromal tumor samples.

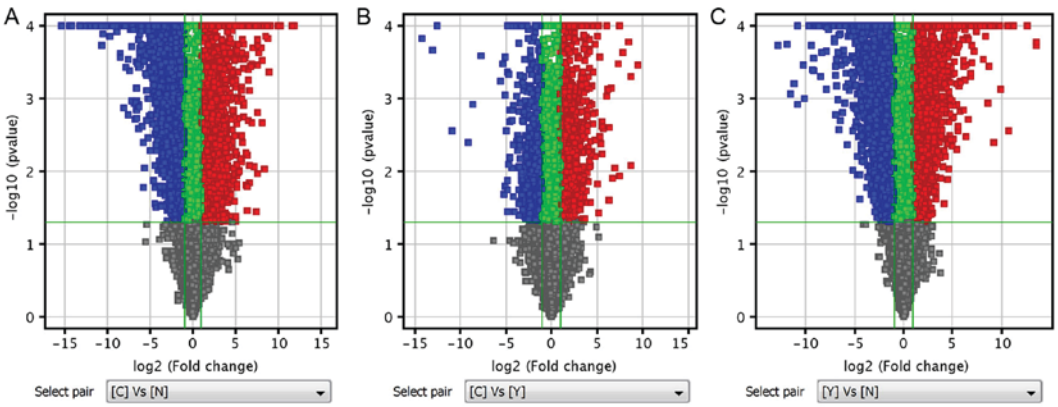

Figure 1. Volcano plot analysis. (A) Volcano plot analysis of group C vs. N. (B) Volcano plot analysis of group C vs. Y. (C) Volcano plot analysis of group Y vs. N. The Volcano plots contain differentially expressed mRNAs and lncRNAs and indicate the full pictures of mRNAs and lncRNAs. The abscissa represents the difference between the two data sets following log2 conversion and the ordinate represents the -log10 (P-value) calculated by unpaired Student's t-test. Red dots represent significantly upregulated molecules, blue dots represent significantly downregulated molecules, green dots represent the molecules changed, but with a fold-change <2. N, normal gastric tissue samples; Y, primary gastrointestinal stromal tumor samples; C, imatinib mesylate-resistant gastrointestinal stromal tumor samples; lncRNA, long non-coding RNA.

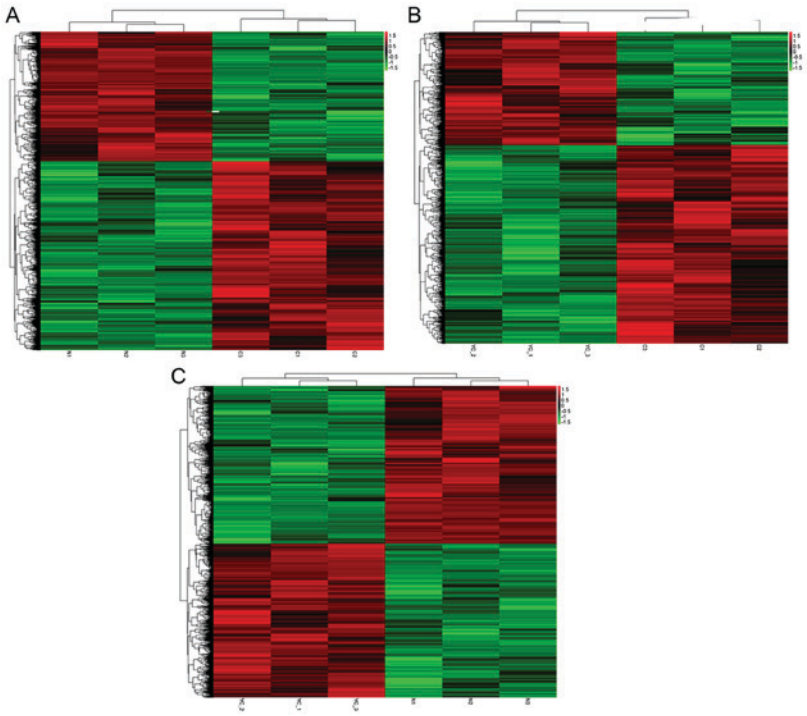

Figure 2. Cluster analysis of differentially expressed mRNAs and long non-coding RNAs. (A) Cluster analysis of imatinib mesylate-resistant gastrointestinal stromal tumor samples vs. normal gastric tissue samples. (B) Cluster analysis of imatinib mesylate-resistant gastrointestinal stromal tumor samples vs. primary gastrointestinal stromal tumor samples. (C) Cluster analysis of primary gastrointestinal stromal tumor samples vs. normal gastric tissue samples.

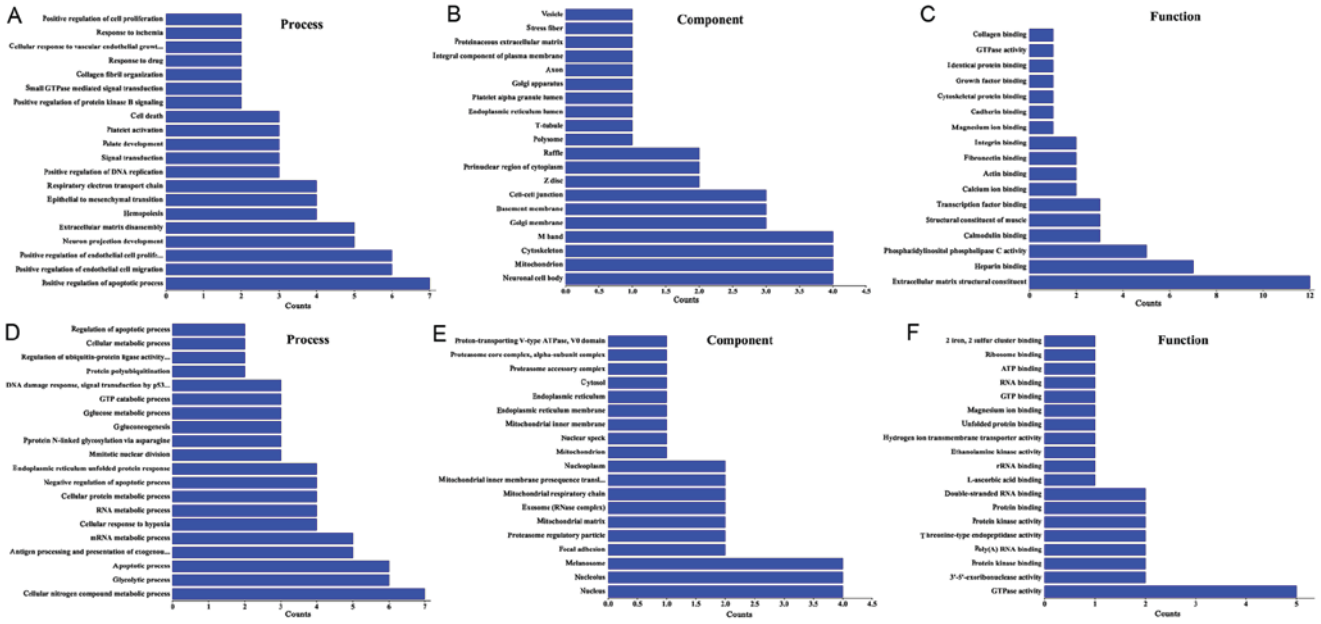

Figure 3. GO enrichment analysis. (A-C) GO enrichment analysis of differentially expressed lncRNAs between normal gastric tissue samples and normal gastric tissue samples. (A) Biological process. (B) Cellular component and (C) molecular function analysis. (D-F). GO enrichment analysis of differentially expressed lncRNAs between imatinib mesylate-resistant gastrointestinal stromal tumor samples and primary gastrointestinal stromal tumor samples. (D) Biological process, (E) cellular component and (F) molecular function analysis. GO, Gene Ontology; lncRNA, long non-coding RNA.

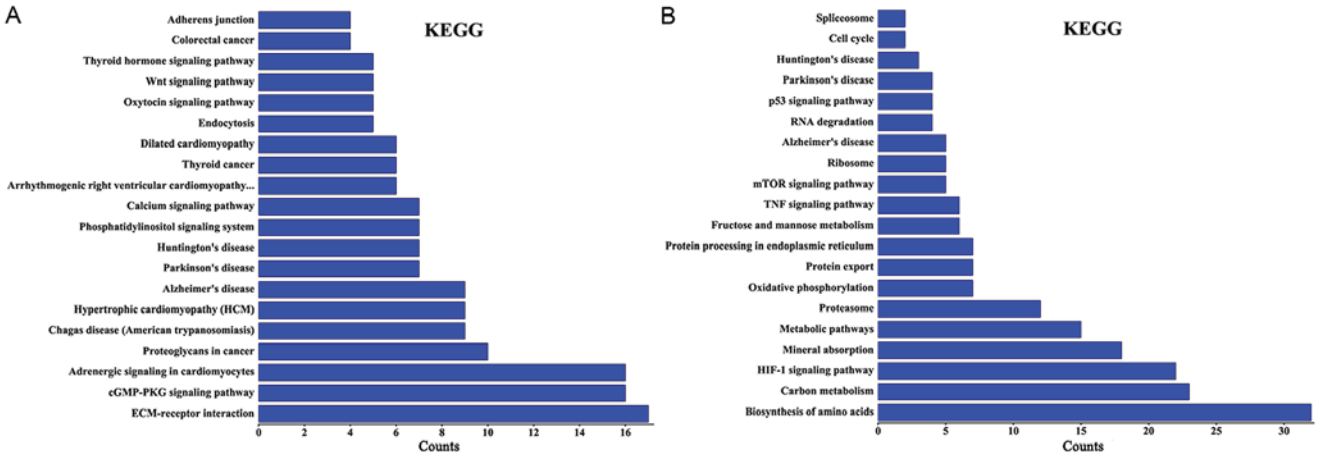

Figure 4. KEGG pathway analysis. (A) KEGG pathway analysis of the differentially expressed lncRNAs between primary gastrointestinal stromal tumor samples and normal gastric tissue samples. (B) KEGG pathway analysis of the differentially expressed lncRNAs between imatinib mesylate-resistant gastrointestinal stromal tumor samples and primary gastrointestinal stromal tumor samples. KEGG, Kyoto Encyclopedia of Genes and Genomes; lncRNA, long non-coding RNA.

Table V. Most highly connected TFs in the long non-coding RNA-TF network when comparing normal gastric tissue samples and primary gastrointestinal stromal tumor samples.

TF	Node frequency, n
E2F1	29
GATA2	1
STAT3	33
RAD21	26
FOXA1	11

TF, transcription factor.

lncRNA function prediction. Using GO enrichment and KEGG pathway analysis the functions of the differentially expressed lncRNAs were predicted. In the GO biological processes classification, a number of differentially expressed lncRNAs in group Y (primary GISTs) compared with group N (normal tissues) were implicated in 'positive regulation of the apoptotic processes', 'extracellular matrix disassembly', 'endothelial cell migration', 'cellular response to vascular endothelial growth factor stimulus', 'DNA replication' and 'endothelial cell proliferation'. Numerous differentially expressed lncRNAs were associated with the following cellular components: 'M band', 'cytoskeleton', 'neuronal cell body', 'mitochondria' and 'cell-cell junctions'. In addition, the differentially expressed lncRNAs were associated with the following molecular

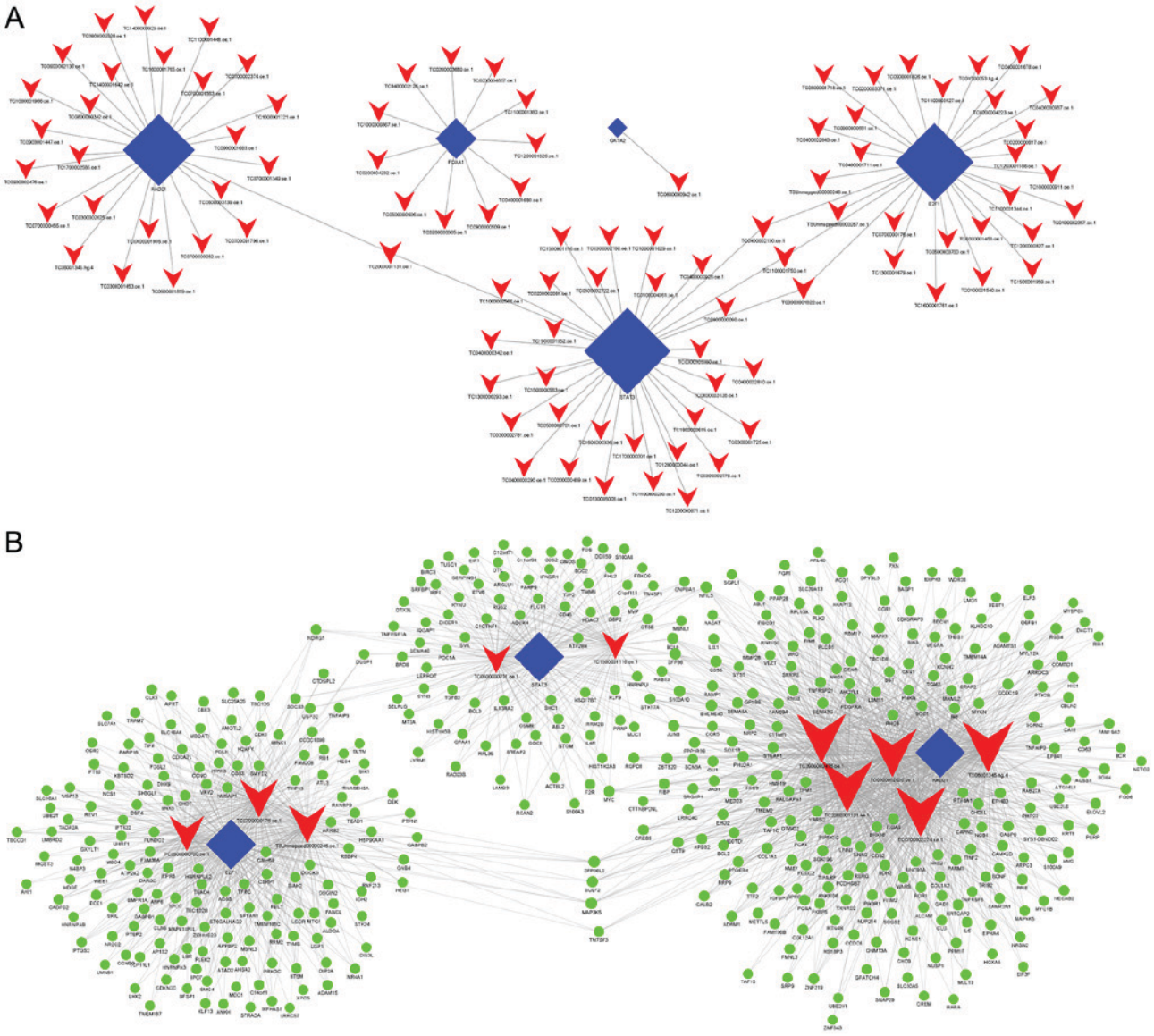

Figure 5. lncRNA-TF and lncRNA-TF-mRNA interaction networks. (A) lncRNA-TF interaction of primary gastrointestinal stromal tumor samples vs. normal gastric tissue samples. There are 100 lncRNA-TF interactions pairs, 5 TFs and 96 lncRNAs in the network. (B) lncRNA-TF-mRNA network analysis of primary gastrointestinal stromal tumor samples vs. normal gastric tissue samples. There are 1,871 interactions pairs, 3 TFs, 10 lncRNAs and 452 target genes in the network. Blue nodes represent TFs, red nodes represent lncRNAs, green nodes represent target genes and the node size is proportional to its outward connection. lncRNA, long non-coding RNA; TF, transcription factor.

function terms: 'Extracellular matrix structural constituents', 'heparin binding', 'actin binding', 'fibronectin binding' and 'phosphatidylinositol phospholipase C activity' (Fig. 3A-C).

GO enrichment analysis was also performed for the differentially expressed lncRNAs identified between group C (secondary imatinib mesylate-resistant GISTs) and group Y (primary GISTs). It was identified that the lncRNAs were enriched in the following processes: 'Cellular nitrogen compound metabolism', 'apoptosis', 'glycolysis and glucose metabolism', and 'protein polyubiquitination'. In addition, the lncRNAs were enriched in the following cellular components: 'Nucleus', 'endoplasmic reticulum', 'membrane', 'nucleolus', 'melanosome' and 'proteasome regulatory particle'. Furthermore, the lncRNAs were associated with 'GTPase activity', 'threonine-type endopeptidase activity', 'ribosomal structural constituents', 'protein kinase activity' and 'two iron, two sulfur cluster binding' (Fig. 3D-F).

Using KEGG pathway analysis, it was revealed that the differentially expressed lncRNAs in group Y (primary GISTs tissues) compared with group N (normal tissues) were enriched in the 'cyclic guanosine monophosphate-protein kinase cGMP-dependent 1 (cGMP-PKG) signaling pathways', 'extracellular matrix-receptor interactions', 'thyroid hormone signaling pathways', 'phosphatidylinositol signaling systems' and 'calcium signaling pathways'. The activation of these signaling pathways through the differentially expressed lncRNAs may be associated with GIST occurrence. When group C (imatinib mesylate-resistant GISTs) was compared with group Y (primary GISTs), the differentially expressed lncRNAs were enriched in the 'hypoxia-inducible factor-1 (HIF-1) signaling pathway', 'amino acids biosynthesis', 'metabolic pathways', the 'tumor necrosis factor (TNF) signaling pathway', the 'mammalian target of rapamycin (mTOR) signaling pathway' and the 'p53 signaling pathway' (Fig. 4).

Table VI. Top ten most highly connected lncRNAs in the lncRNA-transcription factor-mRNA network when comparing normal gastric tissue samples and primary gastrointestinal stromal tumor samples.

Probe set ID	lncRNA	Regulation	Node frequency, n
TC2000001131.oe.1	lnc-SLA2-2	Downregulated	184
TC08001345.hg.4	ZFHX4-AS1	Upregulated	181
TC0700002374.oe.1	lnc-GNAT3-4	Downregulated	178
TC0900002476.oe.1	lnc-UBAC1-2	Downregulated	175
TC0300002625.oe.1	lnc-IMPG2-3	Downregulated	169
TC0700000176.oe.1	lnc-BZW2-2	Upregulated	124
TSUnmapped00000246.oe.1	lnc-C11orf89-3	Upregulated	123
TC0500000700.oe.1	lnc-F2R-4	Upregulated	111
TC0500000701.oe.1	lnc-F2R-3	Upregulated	80
TC1500001116.oe.1	lnc-SYNM-5	Downregulated	78

lncRNA, long non-coding RNA.

Certain lncRNAs may serve a role in the activation of these signaling pathways and may be associated with secondary resistance to imatinib.

lncRNA-TF-mRNA network analysis. Using the hypergeometric distribution calculation, a number of lncRNA-TF associations were identified for each differentially expressed lncRNA. Each lncRNA-TF association was the result of multiple gene enrichment. A two-association network graph was constructed of the lncRNA-TF associations for the top 100 differentially expressed lncRNAs. In addition, a three-association network graph was constructed using the top 10 differentially expressed lncRNAs.

When comparing group Y (primary GISTs) with group N (normal tissues), it was identified that E2F1, GATA2, STAT3, RAD21 and FOXA1 were the most highly connected TFs, which indicates these TFs may be associated with the occurrence of GISTs (Fig. 5A; Table V).

Furthermore, when comparing group Y (primary GISTs) with group N (normal tissues), it was revealed that lnc-SLA2-2, ZFHX4-AS1, lnc-GNAT3-4, lnc-UBAC1-2, lnc-IMPG2-3, lnc-BZW2-2, lnc-C11orf89-3, lnc-F2R-4, lnc-F2R-3 and lnc-SYNM-5 were the most highly connected lncRNAs (Fig. 5B; Table VI). This suggests these lncRNAs may be associated with the occurrence of GISTs.

When group C was compared with group Y (primary GISTs), it was identified that TBP, USF1, TAF1, NRF1, USF2, MAX, E2F4, EBF1, KAT2A, GABPA, SMARCA4, STAT3, BCLAF1, E2F6, and MYC were the most highly connected TFs (Fig. 6; Table VII). This indicates that these TFs may be associated with secondary resistance to imatinib.

Additionally, when group C (imatinib mesylate-resistant GISTs) was compared with group Y (primary GISTs), it was revealed that NONHSAG008085//lnc-RAG2-5//RP11-159D8.2, lnc-GZMA-2, lnc-KIAA1462-10, lnc-NAIP-5, lnc-DNAJC6-2, lnc-IMMT-3, lnc-CEP170-11, lnc-LNPEP-5, lnc-C11orf82-6 and lnc-FNDC5-3 were the most highly connected lncRNAs. These lncRNAs may be associated with secondary resistance to imatinib (Fig. 7; Table VIII).

Table VII. Most highly connected TFs in the long non-coding RNA-TF network when comparing primary gastrointestinal stromal tumor samples with imatinib mesylate-resistant gastrointestinal stromal tumor samples.

TF	Node frequency, n
TBP	7
USF1	2
TAF1	16
NRF1	7
USF2	1
MAX	15
E2F4	1
EBF1	1
KAT2A	1
GABPA	1
SMARCA4	1
STAT3	35
BCLAF1	1
E2F6	2
MYC	9

TF, transcription factor.

The differentially expressed lncRNAs identified when comparing group C (imatinib mesylate-resistant GISTs) with group Y (primary GISTs) were compared with lncRNAs associated with the HIF-1 pathway and lncRNAs were filtered out with multiple differences <4. An lncRNA-TF-mRNA network was constructed, which revealed that lnc-DNAJC6-2 was highly associated with the HIF-1 pathway (Figs. 8 and 9; Table IX).

Quantitative analysis. During RT-qPCR, the melting curve for each gene was a single peak and the specificity of the PCR amplification was high. The data from three independent experiments were consistent and all gene validation

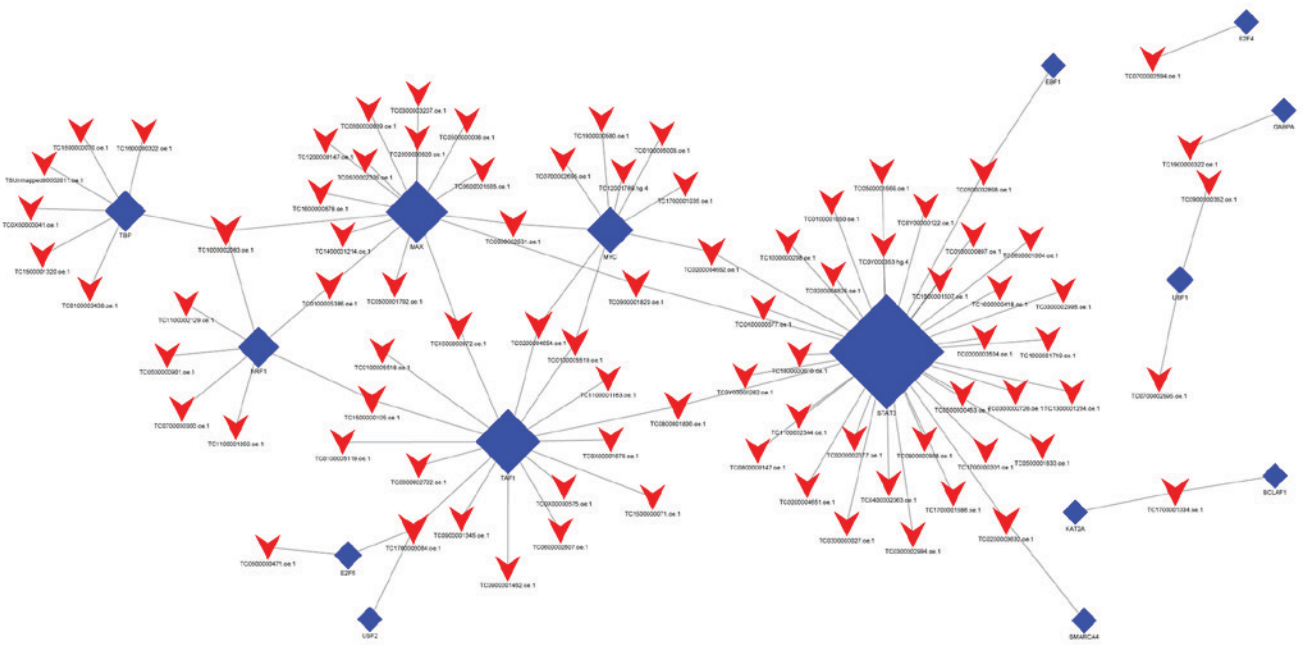

Figure 6. lncRNA-TF network analysis of imatinib mesylate-resistant gastrointestinal stromal tumor samples vs. primary gastrointestinal stromal tumor samples. There are 100 lncRNA-TF interactions pairs, 15 TFs and 84 lncRNAs in the network. Blue nodes represent TFs, red nodes represent lncRNAs and the node size is proportional to its outward connection. lncRNA, long non-coding RNA; TF, transcription factor.

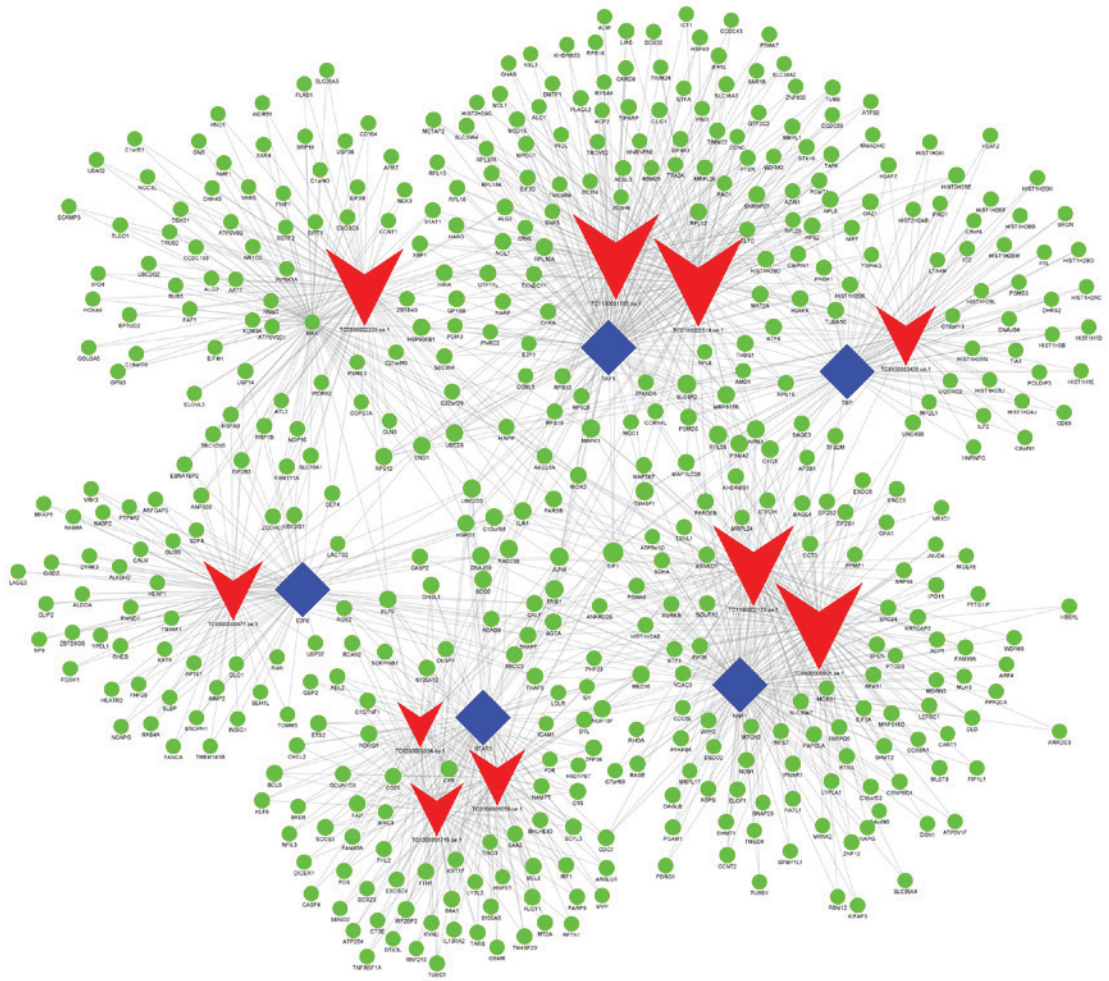

Figure 7. lncRNA-TF-mRNA network analysis of imatinib mesylate-resistant gastrointestinal stromal tumor samples vs. primary gastrointestinal stromal tumor samples. There are 1,356 interactions pairs, 6 TFs, 10 lncRNAs and 465 mRNAs in the network. Transcription factor MAX was also included in targeted genes and indicated with green dots. Blue nodes represent TFs, red nodes represent lncRNAs, green nodes represent target genes and the node size is proportional to its outward connection. lncRNA, long non-coding RNA; TF, transcription factor.

Table VIII. Top ten most highly connected lncRNAs differences in the lncRNA-transcription factor-mRNA network when comparing primary gastrointestinal stromal tumor samples with imatinib mesylate-resistant gastrointestinal stromal tumor samples.

Probe set ID	lncRNA	Regulation	Node frequency, n
TC1100002129.oe.1	NONHSAG008085//lnc-RAG2-5//RP11-159D8.2	Upregulated	96
TC0500000471.oe.1	lnc-GZMA-2	Upregulated	65
TC1000001719.oe.1	lnc-KIAA1462-10	Downregulated	56
TC0500002335.oe.1	lnc-NAIP-5	Downregulated	91
TC0100001050.oe.1	lnc-DNAJC6-2	Upregulated	60
TC0200003534.oe.1	lnc-IMMT-3	Downregulated	45
TC0100005519.oe.1	lnc-CEP170-11	Downregulated	107
TC0500000901.oe.1	lnc-LNPEP-5	Upregulated	105
TC1100001163.oe.1	lnc-C11orf82-6	Upregulated	103
TC0100003438.oe.1	lnc-FNDC5-3	Upregulated	65

lncRNA, long non-coding RNA.

Table IX. Targets of long non-coding-DNAJC6-2 in the hypoxia-inducible factor-1 pathway.

Target	mRNA/TF
ATF3	TF
ENO1	mRNA
RPS6KB2	mRNA
SMARCA4	TF
HMOX1	mRNA
CEBPB	TF
NR3C1	TF
MYC	TF
LDHA	mRNA
MAX	TF
MYC	TF
SMARCA4	TF
ALDOA	mRNA

TF, transcription factor.

experiments were successful. The data were analyzed by the $2^{-\Delta\Delta Cq}$ method and the expression of the 6 differentially expressed lncRNAs by random selection were consistent with the microarray results (Fig. 10; Table X). In comparison between Group C and Y, four lncRNAs, including lnc-TERT-2, lnc-OMD-1, lnc-ATP7A-2 and lnc-RERE-4, were significantly highly expressed in Group C, while two lncRNAs, lnc-TCF4-6 and lnc-SNRPN-2, were significantly highly expressed in Group Y.

Discussion

The current study recruited 9 patients, including 3 patients without cancer (group N), 3 patients with primary GISTs (group Y) and 3 patients with GISTs that were secondary resistant to IM (group C). Samples for microarray experiments were obtained. As expected, differential expression of lncRNAs was observed for each paired sample. This included 2,250 lncRNAs in group Y vs. group N, 2,209 lncRNAs in group C vs. group N and 922 lncRNAs in group C vs. group Y. This suggests that lncRNAs may serve as biomarkers for GISTs and further studies may lead to the development of novel therapies.

Following the identification of differentially expressed lncRNAs, GO enrichment and KEGG pathway analyses were performed to assess potential functions and mechanisms of these factors. Based on GO enrichment and KEGG pathway analysis of the differentially expressed lncRNAs between group Y and group C, the HIF-1 signaling pathway result is notable. For a number of years it has been understood that intratumoral hypoxia is often associated with resistance to therapy and a poor prognosis (20,21). HIF-1 is considered to be a sequence-specific DNA-binding TF; its stability is regulated by oxygen and it can control the transcription of target genes under hypoxic conditions by combining with HIF-1β. The rapid proliferation of tumor cells leads to insufficient blood supply, resulting in a hypoxic environment. Therefore, HIF-1 is often overexpressed in tumor tissues. Tumor hypoxia has been demonstrated to be associated with therapy resistance in drug-based treatments and radiation therapies (20,22-28). It has been identified that HIF-1 can modulate >200 genes that are associated with cell cycle arrest, proliferation, apoptosis, survival, metabolism, DNA repair and drug efflux. This results in drug resistance to chemicals and radiation (29-31). Investigating lncRNAs that target the HIF-1 pathway may identify a novel cancer treatment strategy (32). In the current study, lnc-DNAJC6-2 was identified to be associated with the HIF-1 pathway, this lncRNA may target the expression of TFs, including ATF3, SMARCA4, CEBPB, NR3C1, MYC, MAX, MYC and SMARCA4, and affect ENO1, RPS6KB2, HMOX1, LDHA and ALDOA. An important role of lnc-DNAJC6-2 has been demonstrated in the progression of hepatocellular carcinoma (HCC) and lnc-DNAJC6-2 has

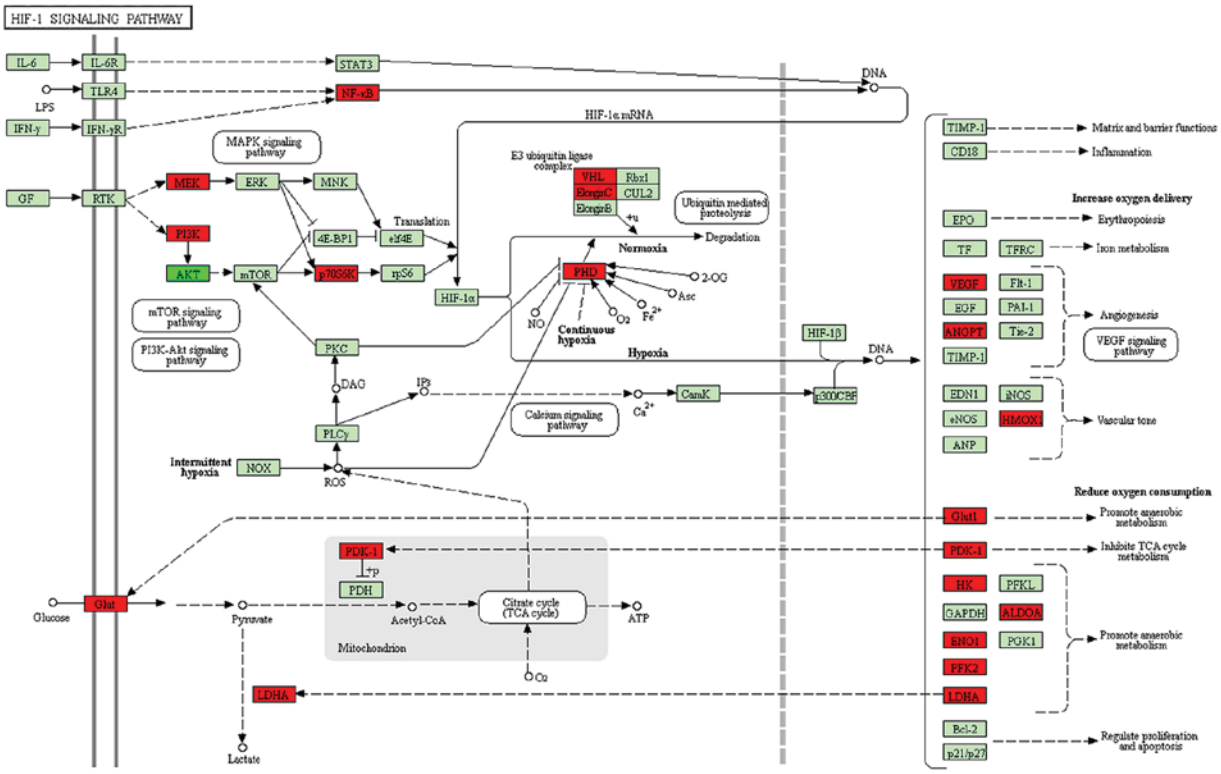

Figure 8. Differentially expressed mRNAs in the HIF-1 pathway. Red nodes indicate mRNA overexpression, bright green nodes indicate low mRNA expression and light green nodes indicate no difference in mRNA expression. HIF-1, hypoxia-inducible factor-1.

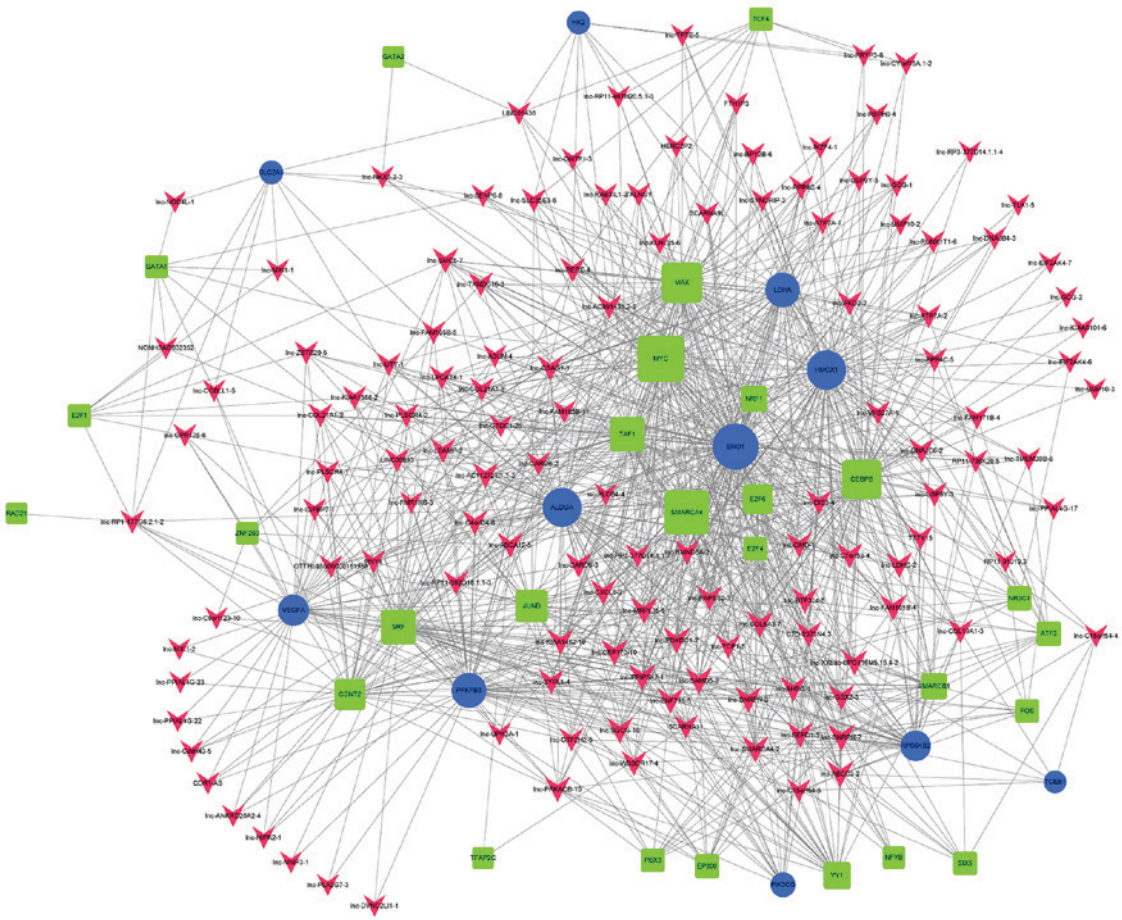

Figure 9. lncRNA-TF-mRNA network analysis of the hypoxia-inducible factor-1 pathway. Green nodes represent TFs, red nodes represent lncRNAs and blue nodes represent target genes. lncRNA, long non-coding RNA; TF, transcription factor.

Table X. lncRNA expression levels validated by reverse transcription-quantitative polymerase chain reaction.

lncRNA	Mean of YC	Mean of C	SD of YC	SD of C	P-value
lnc-TERT-2	1.009753629	10.90599007	0.166744554	5.161105469	0.0294
lnc-OMD-1	1.031618183	4.016359625	0.311642071	1.120932182	0.0113
lnc-ATP7A-2	1.006134328	7.556070844	0.132794714	0.989899179	0.0003
lnc-TCF4-6	1.003862861	0.157260729	0.109907251	0.105244389	0.0006
lnc-RERE-4	1.008350471	14.39198375	0.154486795	2.278985694	0.0005
lnc-SNRPN-2	1.007281843	0.310708716	0.152063775	0.131714432	0.0039

YC, primary gastrointestinal stromal tumor samples; C, imatinib mesylate-resistant gastrointestinal stromal tumor samples; SD, standard deviation; lncRNA, long non-coding RNA.

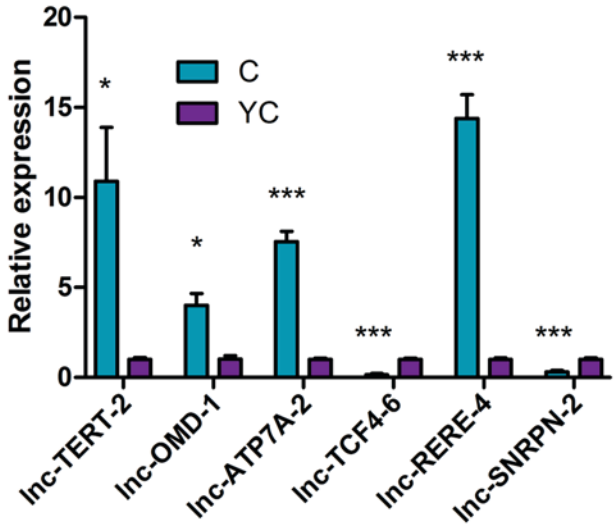

Figure 10. Reverse transcription-quantitative polymerase chain reaction validation of 6 lncRNAs. *P<0.05 and ***P<0.001 vs. YC. C, imatinib mesylate-resistant gastrointestinal stromal tumor samples; YC, primary gastrointestinal stromal tumor samples; lncRNA, long non-coding RNA.

been implicated as a marker of poor outcome in HCC (33). The current study only performed gene sequencing and data analysis. A larger sample size is required to validate the current results. Additionally, further elucidation and functional verification is required to investigate additional mechanisms of imatinib mesylate resistance.

In the lncRNA-TF-mRNA network analysis, lnc-SLA2-2, ZFHX4-AS1, lnc-GNAT3-4, lnc-UBAC1-2, lnc-IMPG2-3, lnc-BZW2-2, lnc-C11orf89-3, lnc-F2R-4, lnc-F2R-3 and lnc-SYNM-5 were the most highly connected lncRNAs. These lncRNAs may modulate the expression of TFs, including E2F1, STAT3 and RAD21, and this may be associated with the occurrence of GISTs. Furthermore, NONHSAG008085//lnc-RAG2-5//RP11-159D8.2,lnc-GZMA-2, lnc-KIAA1462-10, lnc-NAIP-5, lnc-DNAJC6-2, lnc-IMMT-3, lnc-CEP170-11, lnc-LNPEP-5, lnc-C11orf82-6 and lnc-FNDC5-3 were the most highly connected lncRNAs with the expression of TFs, including TBP, TAF1, NRF1, MAX, STAT3 and E2F6. This may be associated with secondary resistance to imatinib.

In conclusion, following resistance to IM, few therapeutic options are available for GISTs. Therefore, there is an urgent requirement to identify the mechanisms of drug resistance. The findings of the current study indicate that lncRNAs may serve active roles in the occurrence of GISTs and secondary resistance to imatinib. Certain lncRNAs, including lnc-DNAJC6-2 may modulate the HIF-1 signaling pathway. Therefore, the identified lncRNAs may prove to be important targets for treating secondary imatinib mesylate resistance in GISTs.

Acknowledgements

No applicable.

Funding

This study was supported by the Natural Science Foundation of Zhejiang Province (grant no. LY15H160060) and the Science and Technology Bureau of Wenzhou of Zhejiang Province (grant no. Y20140364).

Availability of data and materials

The datasets used during the present study are available from the corresponding author upon reasonable request.

Authors' contributions

JY, DC and XC conceived the idea. JY and DC performed the experiments. XS, QD, TW and ZD analyzed the data. XC wrote the manuscript. All authors have read and approved the final version of the manuscript.

Ethics approval and consent to participate

This study was approved by the Ethics Committee of The First Affiliated Hospital of Wenzhou Medical University.

Patient consent for publication

The patient consented for the publication of any associated data and accompanying images.

Competing interests

The authors declare that they have no competing interests.

References

1. Hirota S, Isozaki K, Moriyama Y, Hashimoto K, Nishida T, Ishiguro S, Kawano K, Hanada M, Kurata A, Takeda M, *et al*: Gain-of-function mutations of c-kit in human gastrointestinal stromal tumors. Science 279: 577-580, 1998.
2. Nishida T and Hirota S: Biological and clinical review of stromal tumors in the gastrointestinal tract. Histol Histopathol 15: 1293-1301, 2000.
3. Verweij J, Casali PG, Zalcberg J, LeCesne A, Reichardt P, Blay JY, Issels R, van Oosterom A, Hogendoorn PC, Van Glabbeke M, *et al*: Progression-free survival in gastrointestinal stromal tumours with high-dose imatinib: Randomised trial. Lancet 364: 1127-1134, 2004.
4. Heinrich MC, Corless CL, Demetri GD, Blanke CD, von Mehren M, Joensuu H, McGreevey LS, Chen CJ, Van den Abbeele AD, Druker BJ, *et al*: Kinase mutations and imatinib response in patients with metastatic gastrointestinal stromal tumor. J Clin Oncol 21: 4342-4349, 2003.
5. Kretz M, Siprashvili Z, Chu C, Webster DE, Zehnder A, Qu K, Lee CS, Flockhart RJ, Groff AF, Chow J, *et al*: Control of somatic tissue differentiation by the long non-coding RNA TINCR. Nature 493: 231-235, 2013.
6. Klattenhoff CA, Scheuermann JC, Surface LE, Bradley RK, Fields PA, Steinhauser ML, Ding H, Butty VL, Torrey L, Haas S, *et al*: Braveheart, a long noncoding RNA required for cardiovascular lineage commitment. Cell 152: 570-583, 2013.
7. Lee NK, Lee JH, Kim WK, Yun S, Youn YH, Park CH, Choi YY, Kim H and Lee SK: Promoter methylation of PCDH10 by HOTAIR regulates the progression of gastrointestinal stromal tumors. Oncotarget 7: 75307-75318, 2016.
8. Mohammad F, Mondal T, Guseva N, Pandey GK and Kanduri C: Kcnq1ot1 noncoding RNA mediates transcriptional gene silencing by interacting with Dnmt1. Development 137: 2493-2499, 2010.
9. Sun L, Goff LA, Trapnell C, Alexander R, Lo KA, Hacisuleyman E, Sauvageau M, Tazon-Vega B, Kelley DR, Hendrickson DG, *et al*: Long noncoding RNAs regulate adipogenesis. Proc Natl Acad Sci USA 110: 3387-3392, 2013.
10. Pandey GK, Mitra S, Subhash S, Hertwig F, Kanduri M, Mishra K, Fransson S, Ganeshram A, Mondal T, Bandaru S, *et al*: The risk-associated long noncoding RNA NBAT-1 controls neuroblastoma progression by regulating cell proliferation and neuronal differentiation. Cancer Cell 26: 722-737, 2014.
11. Gupta RA, Shah N, Wang KC, Kim J, Horlings HM, Wong DJ, Tsai MC, Hung T, Argani P, Rinn JL, *et al*: Long non-coding RNA HOTAIR reprograms chromatin state to promote cancer metastasis. Nature 464: 1071-1076, 2010.
12. Niinuma T, Suzuki H, Nojima M, Nosho K, Yamamoto H, Takamaru H, Yamamoto E, Maruyama R, Nobuoka T, Miyazaki Y, *et al*: Upregulation of miR-196a and HOTAIR drive malignant character in gastrointestinal stromal tumors. Cancer Res 72: 1126-1136, 2012.
13. Lee NK, Lee JH, Kim WK, Yun S, Youn YH, Park CH, Choi YY, Kim H and Lee SK: Promoter methylation of PCDH10 by HOTAIR regulates the progression of gastrointestinal stromal tumors. Oncotarget 7: 75307-75318, 2016.
14. Lai S, Wang G, Cao X, Luo X, Wang G, Xia X, Hu J and Wang J: KIT over-expression by p55PIK-PI3K leads to imatinib-resistance in patients with gastrointestinal stromal tumors. Oncotarget 7: 1367-1379, 2016.
15. Li J, Dang Y, Gao J, Li Y, Zou J and Shen L: PI3K/AKT/mTOR pathway is activated after imatinib secondary resistance in gastrointestinal stromal tumors (GISTs). Med Oncol 32: 111, 2015.
16. Xiao Y, Jiao C, Lin Y, Chen M, Zhang J, Wang J and Zhang Z: lncRNA UCA1 contributes to imatinib resistance by acting as a ceRNA against miR-16 in chronic myeloid leukemia cells. DNA Cell Biol 36: 18-25, 2017.
17. Wang H, Li Q, Tang S, Li M, Feng A, Qin L, Liu Z and Wang X: The role of long noncoding RNA HOTAIR in the acquired multi-drug resistance to imatinib in chronic myeloid leukemia cells. Hematology 22: 208-216, 2017.
18. Cao K, Li M, Miao J, Lu X, Kang X, Zhu H, Du S, Li X, Zhang Q, Guan W, *et al*: CCDC26 knockdown enhances resistance of gastrointestinal stromal tumor cells to imatinib by interacting with c-KIT. Am J Transl Res 10: 274-282, 2018.
19. Livak KJ and Schmittgen TD: Analysis of relative gene expression data using real-time quantitative PCR and the 2(-Delta Delta C(T)) method. Methods 25: 402-408, 2001.
20. Semenza GL: Targeting HIF-1 for cancer therapy. Nat Rev Cancer 3: 721-732, 2003.
21. Lin SC, Liao WL, Lee JC and Tsai SJ: Hypoxia-regulated gene network in drug resistance and cancer progression. Exp Biol Med (Maywood) 239: 779-792, 2014.
22. Keith B, Johnson RS and Simon MC: HIF1α and HIF2α: Sibling rivalry in hypoxic tumour growth and progression. Nat Rev Cancer 12: 9-22, 2011.
23. Rohwer N and Cramer T: Hypoxia-mediated drug resistance: Novel insights on the functional interaction of HIFs and cell death pathways. Drug Resist Updat 14: 191-201, 2011.
24. Harris AL: Hypoxia-a key regulatory factor in tumour growth. Nat Rev Cancer 2: 38-47, 2002.
25. Nurwidya F, Takahashi F, Minakata K, Murakami A and Takahashi K: From tumor hypoxia to cancer progression: The implications of hypoxia-inducible factor-1 expression in cancers. Anat Cell Biol 45: 73-78, 2012.
26. Semenza GL: Defining the role of hypoxia-inducible factor 1 in cancer biology and therapeutics. Oncogene 29: 625-634, 2010.
27. Bristow RG and Hill RP: Hypoxia and metabolism. Hypoxia, DNA repair and genetic instability. Nat Rev Cancer 8: 180-192, 2008.
28. Nurwidya F, Takahashi F, Minakata K, Murakami A and Takahashi K: From tumor hypoxia to cancer progression: The implications of hypoxia-inducible factor-1 expression in cancers. Anat Cell Biol 45: 73, 2012.
29. Holmquist-Mengelbier L, Fredlund E, Löfstedt T, Noguera R, Navarro S, Nilsson H, Pietras A, Vallon-Christersson J, Borg A, Gradin K, *et al*: Recruitment of HIF-1alpha and HIF-2alpha to common target genes is differentially regulated in neuroblastoma: HIF-2alpha promotes an aggressive phenotype. Cancer Cell 10: 413-423, 2006.
30. Kaelin WG Jr: The von Hippel-Lindau tumour suppressor protein: O2 sensing and cancer. Nat Rev Cancer 8: 865-873, 2008.
31. Bertout JA, Majmundar AJ, Gordan JD, Lam JC, Ditsworth D, Keith B, Brown EJ, Nathanson KL and Simon MC: HIF2alpha inhibition promotes p53 pathway activity, tumor cell death, and radiation responses. Proc Natl Acad Sci USA 106: 14391-14396, 2009.
32. Shih JW and Kung HJ: Long non-coding RNA and tumor hypoxia: New players ushered toward an old arena. J Biomed Sci 24: 53, 2017.
33. Yang T, Li XN, Li XG, Li M and Gao PZ: DNAJC6 promotes hepatocellular carcinoma progression through induction of epithelial-mesenchymal transition. Biochem Biophys Res Commun 455: 298-304, 2014.